Inorganic Chemistry

Article

pubs.acs.org/IC

Porous Ionic Crystals Modified by Post-Synthesis of $K_2[Cr_3O(OOCH)_6(etpy)_3]_2[\alpha\text{-}SiW_{12}O_{40}]\cdot 8H_2O$ through Single-Crystal-to-Single-Crystal Transformation

Sayaka Uchida,[†] Eri Takahashi, and Noritaka Mizuno*

Department of Applied Chemistry, School of Engineering, The University of Tokyo, 7-3-1, Hongo, Bunkyo-ku, Tokyo 113-8656

Supporting Information

ABSTRACT: Post-synthesis modification of a porous ionic crystal proceeded via two steps (acid treatment followed by ion-exchange) in an aqueous solution and a single-crystal-to-single-crystal manner. Compound $K_2[Cr_3O(OOCH)_6(etpy)_3]_2[\alpha\text{-}SiW_{12}O_{40}]\cdot 8H_2O$ (etpy = 4-ethylpyridine) [**1a**] is a porous ionic crystal with one-dimensional channels, which can accommodate guests such as water, alcohols, and halocarbons. Crystals of **1a** were immersed in an aqueous HCl solution (acid treatment), and the etpy ligand which was exposed to the one-dimensional channel was removed and exchanged with water. The formula of the resulting compound was $(etpyH^+)_2[Cr_3O(OOCH)_6(etpy)_2(H_2O)]_2[\alpha\text{-}SiW_{12}O_{40}]\cdot 6H_2O$ [**2a**], and K^+ ions, which are potential guest binding sites, were simultaneously removed by this treatment. Reincorporation of K^+ ions was attempted by immersion of **2a** into an aqueous CH_3COOK solution (ion-exchange), and $K_2[Cr_3O(OOCH)_6(etpy)_{2.5}(H_2O)_{0.5}]_2[\alpha\text{-}SiW_{12}O_{40}]\cdot 8H_2O$ [**3a**] was formed. Increase in sorption capacity by the two-step post-synthesis modification was confirmed by sorption isotherms and Monte Carlo-based simulations using water as a probe molecule. The role of K^+ ions as water binding sites was confirmed by water sorption isotherms of alkali metal ion-exchanged compounds.

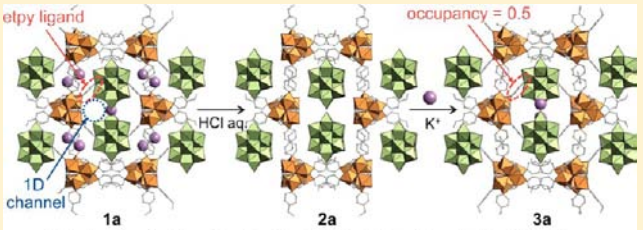

Single-Crystal-to-Single-Crystal Post-Synthesis Modification

INTRODUCTION

Porous crystalline materials such as zeolites and metal−organic frameworks (MOFs) are widely studied because of their unique properties in gas storage, gas separation, heterogeneous catalysis, etc.[1] Post-synthesis modification of porous crystalline materials is a useful strategy to incorporate additional functions that could not be achieved during synthesis.[2,3] In the case of zeolites, transition metal ions such as silver and copper can be incorporated post-synthetically by ion-exchange in an aqueous solution, and the transition metal ion-exchanged zeolites can remove sulfur from fuel[2a] and selectively adsorb and reduce NO_x.[2b] In the case of MOFs, functional groups of organic linkers can be exchanged,[3a] removed,[3b] or extended[3c] post-synthetically. For example, chiral azides are attached post-synthetically onto external alkynes of an organic linker, and the resulting compound catalyzed asymmetric aldol reactions.[3d]

Porous ionic crystals are constructed with molecular anions and cations, which create strong electrostatic fields at internal surfaces that are suitable for accommodating guest molecules.[4] Polyoxometalates (POMs) are anionic nanosized metal−oxygen clusters and suitable inorganic building blocks to form functional ionic crystals because of their discrete structures and interesting acid−base, redox, and photochemical properties.[5] We have reported that POM-based organic−inorganic ionic crystals show high separation ability of mixtures of water/ethanol,[6a] ethylene/ethane,[6b] and CO_2/methane[6c] and catalyze size-selective heterogeneous acid[6d] or oxidation[6e] reactions. While these ionic crystals are easily synthesized by a one-pot reaction in a solution containing the constituent ions, precise prediction and control of structures are difficult because Coulomb interaction works isotropically in a long-range. Based on these considerations, a porous ionic crystal of $K_2[Cr_3O(OOCH)_6(etpy)_3]_2[\alpha\text{-}SiW_{12}O_{40}]\cdot 8H_2O$[6c,7] (etpy = 4-ethylpyridine) [**1a**] was modified by post-synthesis in a single-crystal-to-single-crystal manner. Increase in guest sorption capacity was confirmed by sorption isotherms and Monte Carlo-based simulations using water as a probe molecule.

EXPERIMENTAL METHODS

Syntheses. Single crystals of $K_2[Cr_3O(OOCH)_6(etpy)_3]_2[\alpha\text{-}SiW_{12}O_{40}]\cdot 8H_2O$ [**1a**] were synthesized according to previous reports.[6c,7] Elemental analysis calcd for **1a**: C 14.03, H 1.79, N 1.82, Cr 6.75, K 1.69, Si 0.61, W 47.71; found C 14.07, H 1.90, N 1.64, Cr 6.96, K 1.73, Si 0.67, W 48.03. Single crystals of **1a** (0.1 g, 0.022 mmol) were immersed in 25 mL of 0.3 M HCl_{aq} for 24 h. Dark greenish brown crystals of $(etpyH^+)_2[Cr_3O(OOCH)_6(etpy)_2(H_2O)]_2[\alpha\text{-}SiW_{12}O_{40}]\cdot 6H_2O$ [**2a**] were obtained (yield >90%). Elemental analysis calcd for **2a**: C 14.26, H 1.86, N 1.85, Cr 6.86, K 0.00, Si 0.62, W 48.51; found C 13.86, H 1.95, N 1.69, Cr 7.16, K 0.02, Si 0.66, W 48.48. Single crystals of **2a** (0.1 g, 0.022 mmol) were immersed in a 25 mL aqueous solution containing 2.2 g (0.022 mol) of CH_3COOK for 24 h. Dark brown crystals of

Received: April 5, 2013
Published: July 31, 2013

dx.doi.org/10.1021/ic4008334 | Inorg. Chem. 2013, 52, 9320−9326

$K_2[Cr_3O(OOCH)_6(etpy)_{2.5}(H_2O)_{0.5}]_2[\alpha\text{-}SiW_{12}O_{40}]\cdot 8H_2O$ [**3a**] were obtained (yield >90%). Elemental analysis calcd for **3a**: C 12.45, H 1.67, N 1.54, Cr 6.88, K 1.72, Si 0.62, W 48.65; found C 13.09, H 1.99, N 1.43, Cr 7.24, K 1.63, Si 0.66, W 48.80. Compounds $K_2[Cr_3O(OOCH)_6(etpy)_3]_2[\alpha\text{-}SiW_{12}O_{40}]\cdot 2H_2O$ [**1b**],[6c] $(etpyH^+)_2[Cr_3O(OOCH)_6(etpy)_2(H_2O)]_2[\alpha\text{-}SiW_{12}O_{40}]\cdot 2H_2O$ [**2b**], and $K_2[Cr_3O(OOCH)_6(etpy)_{2.5}(H_2O)_{0.5}]_2[\alpha\text{-}SiW_{12}O_{40}]\cdot 2H_2O$ [**3b**] were formed by the treatments of **1a**, **2a**, and **3a**, respectively, in vacuo or under a dry N_2 flow at 298−303 K. The amounts of water in **1b**−**3b** (2 mol mol^{-1}) were confirmed by thermogravimetry. Water molecules in **1b**−**3b** were completely desorbed by the treatment in vacuo or under a dry N_2 flow at 373 K, while powder XRD patterns showed structure changes after the treatment.

Single Crystal X-ray Structure and Void Space Analyses. X-ray diffraction data were collected at 153 K with CCD 2-D detector by using a Rigaku Saturn diffractometer with graphite monochromated Mo Kα radiation. Data reduction and absorption correction were performed with the HKL2000 package. Structures were solved by the direct method, expanded using Fourier techniques, and refined by full-matrix least-squares against F^2 with the SHELXTL package. Silicon, chromium, and tungsten atoms were refined anisotropically, while carbon, oxygen, and potassium atoms were refined isotropically. Crystal data for **1a** has been reported in refs 6c and 7. Crystal data for **2a**: Monoclinic $C2/c$, a = 30.6226(11) Å, b = 25.9098(8) Å, c = 13.3986(5) Å, β = 104.7305(14)°, V = 10281.4(7) $Å^3$, Z = 4, R1 and wR2 values 0.0818 and 0.2855 ($I > 2\sigma(I)$), respectively. While $etpyH^+$ ions could not be located by the single crystal X-ray structure analysis, the existence was confirmed by elemental analysis. Crystal data for **3a**: Monoclinic $C2/c$, a = 32.0195(4) Å, b = 25.3116(5) Å, c = 13.5808(2) Å, β = 110.5485(6)°, V = 10306.5(3) $Å^3$, Z = 4, R1 and wR2 values 0.0781 and 0.2805 ($I > 2\sigma(I)$), respectively. CCDC 926432 and 926433 contain the CIF data for **2a** and **3a**, respectively. Void space volumes of **1b**−**3b** were calculated and displayed based on contact surface by a crystal structure visualization software Mercury (CCDC) after optimizing the positions of $etpyH^+$ ions and 2 mol mol^{-1} of water of crystallization by MC simulations (see below).

Powder X-ray Diffraction Measurements. Powder X-ray diffraction (XRD) patterns were measured with a XRD-DSCII (Rigaku Corporation) by using Cu Kα radiation (λ = 1.54056 Å, 50 kV−300 mA) at ambient conditions. Diffraction data were collected in the range of 2θ = 3−15° at 0.01° point and 5 s $step^{-1}$. Measurements for **1b**−**3b** were carried out under a dry N_2 flow.

Vapor Sorption Measurements. Vapor sorption isotherms at 298 K were measured with a Belsorp-max (BEL Japan Inc.). Compounds **1a**, **2a**, and **3a** (ca. 0.1 g) were treated in vacuo at 303 K for >3 h to form **1b**, **2b**, and **3b**, respectively. The P_0 values for water, methanol, ethanol, and 1-propanol were 3.17 kPa, 16.9 kPa, 7.89 kPa, and 2.73 kPa, respectively. The P_0 values for dichloromethane and 1,2-dichloropropane were 58.1 and 6.61 kPa, respectively. The sorption equilibrium was judged by the following criterion: ±0.3% of pressure change in 5 min. Cross-sectional areas of alcohols and halocarbons were calculated with the molecular weights and densities of liquids at 298 K assuming spherical shapes and close packings of the molecules in the liquid states.[8]

Monte Carlo-Based Simulations. Monte Carlo (MC) simulations were carried out using the Sorption tool of Materials Studio package (Accelrys Inc.) by the Metropolis MC method with universal forcefield.[9,10] During the MC simulations, positions of all atoms of the hosts (silicododecatungstates, macrocations, K^+ ions, and $etpyH^+$ ions) were fixed, while positions of 2 mol mol^{-1} of water of crystallization were optimized with the water guests. Crystal structures of **1a**−**3a** were used as hosts after removal of water molecules, since powder XRD patterns confirmed that the crystal structures of **1b**−**3b** were analogous to those of **1a**−**3a**. Prior to the MC simulations, partial atomic charges of the hosts were derived from DFT calculations as follows: Template structures (silicododecatungstates and macrocations) were cut out from the crystal structure, and geometrical optimization followed by Mulliken charge analysis[11] were carried out using the Dmol^3 tool[12] of Materials Studio package. GGA-PBE[13] exchange-correlation function was used, electron spins of Cr^{3+} ions were treated in an unrestricted manner, and double-numerical plus polarization (DNP) functions were used as the basis sets for all atoms. Geometrical optimization followed by Mulliken charge analysis[11] was also carried out for $etpyH^+$ ions, and the positions of $etpyH^+$ ions in the unit cell were optimized using the Forcite tool with universal forcefield.[10]

RESULTS AND DISCUSSION

The crystal structure of **1a** is shown in Figure 1a.[6c,7] Compound **1a** possessed a one-dimensional channel with an aperture of 3.5 Å and a void surrounded by etpy ligands. Each space contained one K^+ ion per formula unit. The structure of

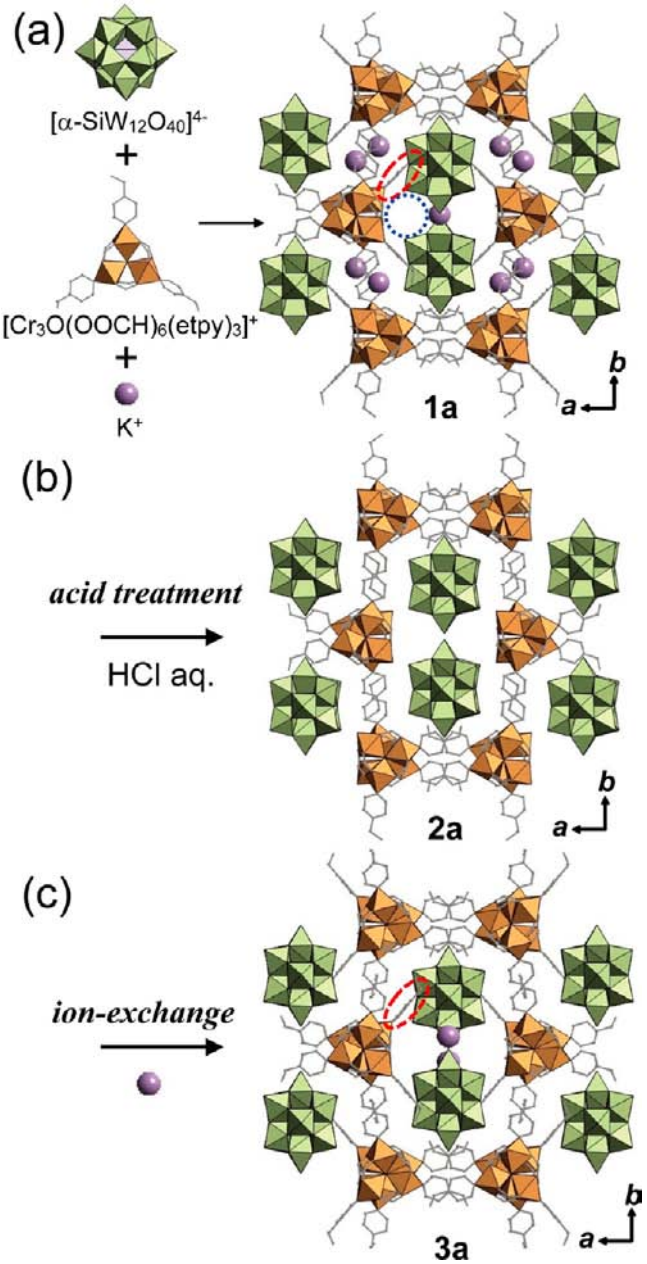

Figure 1. Schematic syntheses and crystal structures of (a) **1a**, (b) **2a**, and (c) **3a**. Light green and orange molecules show silicododecatungstates and macrocations, respectively. Purple spheres show K^+ ions. Blue broken circle in (a) shows the one-dimensional channel. Red broken ovals in (a) and (c) show the etpy ligand exposed to the one-dimensional channel. Site occupancy of this etpy ligand is 0.5 in (c).

dx.doi.org/10.1021/ic4008334 | Inorg. Chem. 2013, 52, 9320−9326

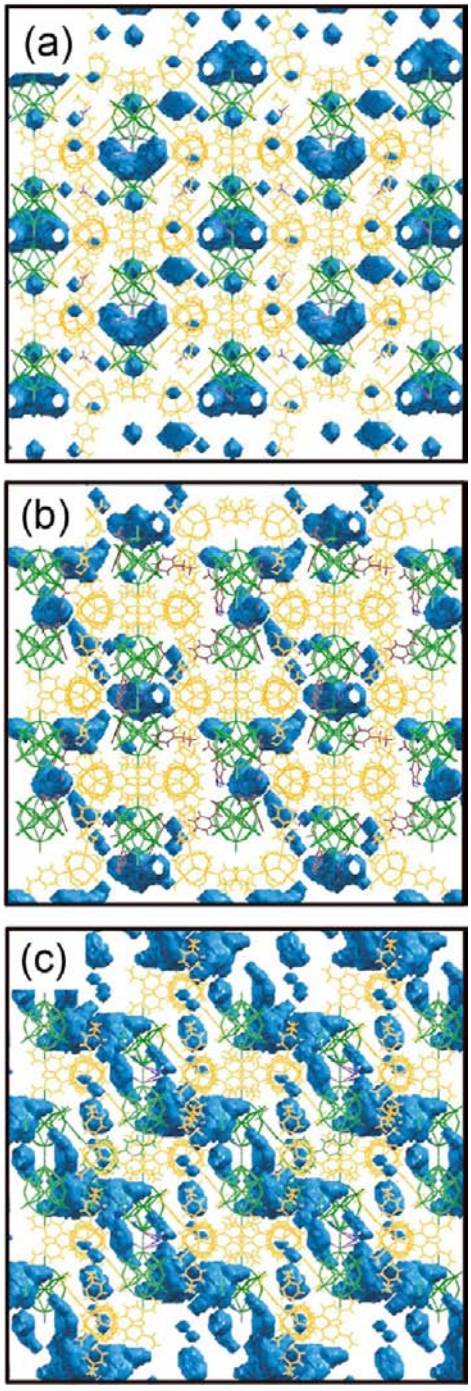

Figure 2. Void spaces in (a) **1b**, (b) **2b**, and (c) **3b**. Void spaces are shown in blue. Green and orange molecules show silicododecatungstates and macrocations, respectively. Brown molecules in (b) show $etpyH^+$ ions. Dark blue and purple sticks show water molecules and K^+ ions, respectively.

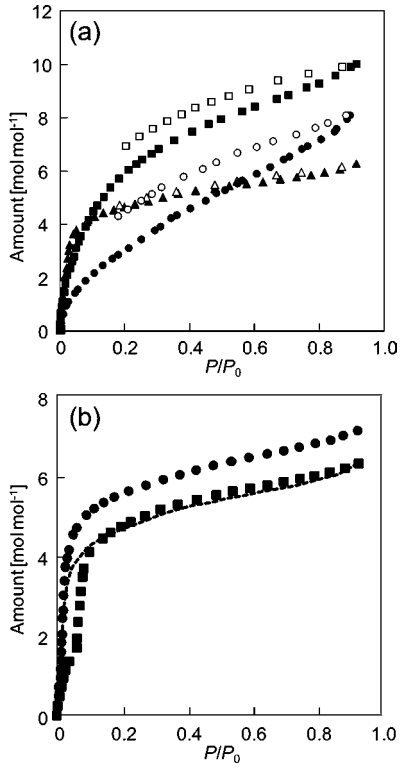

Figure 3. Water sorption−desorption isotherms at 298 K. (a) **1b** (triangle), **2b** (circle), and **3b** (square). Closed and open symbols show the sorption and desorption branches, respectively. (b) **4b** (circle), **5b** (square), and **1b** (broken line).

1a was stabilized by $\pi-\pi$ interaction among neighboring macrocations ($[Cr_3O(OOCH)_6(etpy)_3]^+$). Out of the three terminal etpy ligands of the macrocation, two were involved in the $\pi-\pi$ interaction, and one was exposed to the one-dimensional channel. Therefore, we reached an idea that removal of the latter etpy ligand would enlarge the sorption capacity.

Crystals of **1a** were immersed in an aqueous HCl solution to remove the etpy ligand according to the reaction in eq 1. The crystal structure of the resulting compound after the acid treatment is shown in Figure 1b. The formula of the compound was determined as $(etpyH^+)_2[Cr_3O(OOCH)_6(etpy)_2(H_2O)]_2[\alpha\text{-}SiW_{12}O_{40}]\cdot 6H_2O$ [**2a**] by inductively coupled plasma (ICP), atomic absorption spectrometry (AAS), and CHN elemental analysis. The etpy ligand exposed to the one-dimensional channel was successfully removed and exchanged with water. This ligand-exchange was further supported by the splitting of the $\nu_{asym}(Cr_3O)$ IR band (623 cm^{-1} and 649 cm^{-1}) (Figure S1 in the Supporting Information). Notably, a macrocation containing two kinds of terminal ligands (i.e., etpy and H_2O) could not be selectively synthesized, and a mixture of $[Cr_3O(OOCH)_6(etpy)_{3-n}(H_2O)_n]^+$ (n = 0−3) was formed. Therefore, the macrocation of $[Cr_3O(OOCH)_6(etpy)_2(H_2O)]^+$ in **2a** could be selectively synthesized only by the post-synthesis modification. K^+ ions were simultaneously removed by this treatment, and ethylpyridinium ions ($etpyH^+$ ions) existed as constituent ions. Since K^+ ions probably function as guest binding sites,[6c,7] reincorporation of K^+ ions was attempted by immersion of **2a** into an aqueous CH_3COOK solution, according to the reaction in eq 2.

$$K_2[Cr_3O(OOCH)_6(etpy)_3]_2[\alpha\text{-}SiW_{12}O_{40}] + 2HCl + 2H_2O \rightarrow (etpyH^+)_2[Cr_3O(OOCH)_6(etpy)_2(H_2O)]_2[\alpha\text{-}SiW_{12}O_{40}] + 2KCl \quad (1)$$

dx.doi.org/10.1021/ic4008334 | Inorg. Chem. 2013, 52, 9320−9326

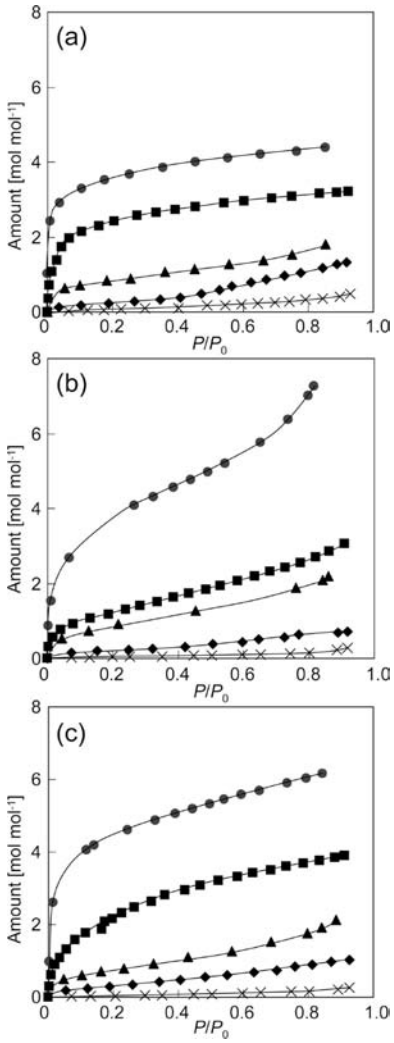

Figure 4. Alcohol and halocarbon sorption isotherms of (a) **1b**, (b) **2b**, and (c) **3b** at 298 K. Circle, square, triangle, diamond, and cross symbols show the data for methanol, ethanol, dichloromethane, 1-propanol, and 1,2-dichloropropane, respectively.

$$(\text{etpyH}^+)_2[\text{Cr}_3\text{O(OOCH)}_6(\text{etpy})_2(\text{H}_2\text{O})]_2[\alpha\text{-SiW}_{12}\text{O}_{40}] + 2\text{CH}_3\text{COOK} \rightarrow \text{K}_2[\text{Cr}_3\text{O(OOCH)}_6(\text{etpy})_{2.5}(\text{H}_2\text{O})_{0.5}]_2[\alpha\text{-SiW}_{12}\text{O}_{40}] + 2\text{CH}_3\text{COOH} + \text{etpy} + \text{H}_2\text{O} \quad (2)$$

The crystal structure of the resulting compound after the ion-exchange treatment is shown in Figure 1c. The formula of the compound was determined as $\text{K}_2[\text{Cr}_3\text{O(OOCH)}_6(\text{etpy})_{2.5}(\text{H}_2\text{O})_{0.5}]_2[\alpha\text{-SiW}_{12}\text{O}_{40}]\cdot 8\text{H}_2\text{O}$ [**3a**] by ICP, AAS, and CHN elemental analysis. K^+ ions were successfully reincorporated into the crystal structure. Two K^+ ions per formula existed in the one-dimensional channel, and these sites were different from that of **1a** (see Supporting Information for details). Single crystal X-ray structure and elemental analyses of **3a** showed that half of etpyH^+ ions in **2a** recoordinated to the macrocation, and the average formula of the macrocation in **3a** was $[\text{Cr}_3\text{O(OOCH)}_6(\text{etpy})_{2.5}(\text{H}_2\text{O})_{0.5}]^+$. Recoordination is probably due to the low solubility of etpy in water. Methanol, ethanol, and acetone were used as solvents for the ion-exchange to improve the solubility of etpy, while **2a** was soluble in these solvents.

Photo images of the post-synthesis modification through single-crystal-to-single-crystal transformation are shown in Figure S3 in the Supporting Information. The solutions (Figure S3a in the Supporting Information) were colorless and transparent, and the morphology of the crystal (Figures S3b–d in the Supporting Information) was basically unchanged, confirming that **2a** and **3a** were not formed by recrystallization of **1a**. Notably, when removal of etpy ligands and reincorporation of K^+ ions were attempted in a single step (i.e., single crystals of **1a** were immersed in HCl_{aq} containing CH_3COOK), elemental analysis and single crystal X-ray structure analysis of the resulting compound gave the formula of $\text{K}_{1.2}(\text{etpyH}^+)_{0.8}[\text{Cr}_3\text{O(OOCH)}_6(\text{etpy})_{2.3}(\text{H}_2\text{O})_{0.7}]_2[\alpha\text{-SiW}_{12}\text{O}_{40}]$, showing that the reincorporation of K^+ ions was incomplete.

Compounds $\text{K}_2[\text{Cr}_3\text{O(OOCH)}_6(\text{etpy})_3]_2[\alpha\text{-SiW}_{12}\text{O}_{40}]\cdot 2\text{H}_2\text{O}$ [**1b**],[6c] $(\text{etpyH}^+)_2[\text{Cr}_3\text{O(OOCH)}_6(\text{etpy})_2(\text{H}_2\text{O})]_2[\alpha\text{-SiW}_{12}\text{O}_{40}]\cdot 2\text{H}_2\text{O}$ [**2b**], and $\text{K}_2[\text{Cr}_3\text{O(OOCH)}_6(\text{etpy})_{2.5}(\text{H}_2\text{O})_{0.5}]_2[\alpha\text{-SiW}_{12}\text{O}_{40}]\cdot 2\text{H}_2\text{O}$ [**3b**] were formed by the treatments of **1a**, **2a**, and **3a**, respectively, in vacuo or under a dry N_2 flow at 298–303 K. Powder XRD of these compounds showed that the crystal structures were maintained after this treatment (Figure S4 in the Supporting Information). Void spaces of **1b**–**3b** are shown in Figure 2. The void space volumes of **1b**, **2b**, and **3b** were 740 Å^3 (6.9%), 505 Å^3 (4.9%), and 1020 Å^3 (9.9%) per unit cell, respectively, and the volumes increased by the post-synthesis from **1b** to **3b**. The void space volume of **2b** was the smallest probably because of the bulky etpyH^+ ions. While most of the voids in **1b** were located in the one-dimensional channel, those in **3b** were extended three-dimensionally by the removal of etpy ligands.

In order to evaluate the sorption capacities of **1b**–**3b**, water sorption–desorption isotherms were measured since the size of water (2.6 Å)[14] is smaller than the channel aperture of **1b** (3.5 Å) and is suitable as a probe. In the water sorption–desorption isotherm of **1b** (Figure 3a), amounts of sorption largely increased at low vapor pressures, a plateau was observed at higher pressures, and the desorption branch overlapped with the sorption branch, which is type I of the IUPAC classification and characteristic of microporous materials.[15] The amounts of sorption for **1b** were 5.4–5.9 mol mol^{-1} at P/P_0 = 0.5–0.8, and the value fairly agreed with that obtained by the thermogravimetric analysis (Figure S5a in the Supporting Information: 5.2 mol mol^{-1} of water sorption at P/P_0 = 0.5 and water desorption in dry He flow at 303 K) and the void volume of **1b** (Figure 2a: 740 Å^3 per unit cell or 6.2 mol mol^{-1} of water). The amounts of sorption for **2b** largely decreased from that for **1b** at low vapor pressures, probably because of the removal of K^+ ions as strong binding sites and/or suppression of water diffusion by etpyH^+ ions. Hystereses were observed in the water sorption isotherms of **2b** and **3b**, suggesting the formation of large spaces.[15] The amounts of sorption for **3b** were similar to those of **1b** at low vapor pressures and about 1.5 times larger than those of **1b** at high vapor pressures. The amounts of sorption for **3b** were 8.0–9.2 mol mol^{-1} at P/P_0 = 0.5–0.8, and the value fairly agreed with that obtained by the thermogravimetric analysis (Figure S5b in the Supporting Information: 8.1 mol mol^{-1} of water sorption at P/P_0 = 0.5 and water desorption in dry He at 303 K) and the void volume of **3b** (Figure 2c: 1020 Å^3 per unit cell or 8.5 mol mol^{-1} of water).

dx.doi.org/10.1021/ic4008334 | Inorg. Chem. 2013, 52, 9320–9326

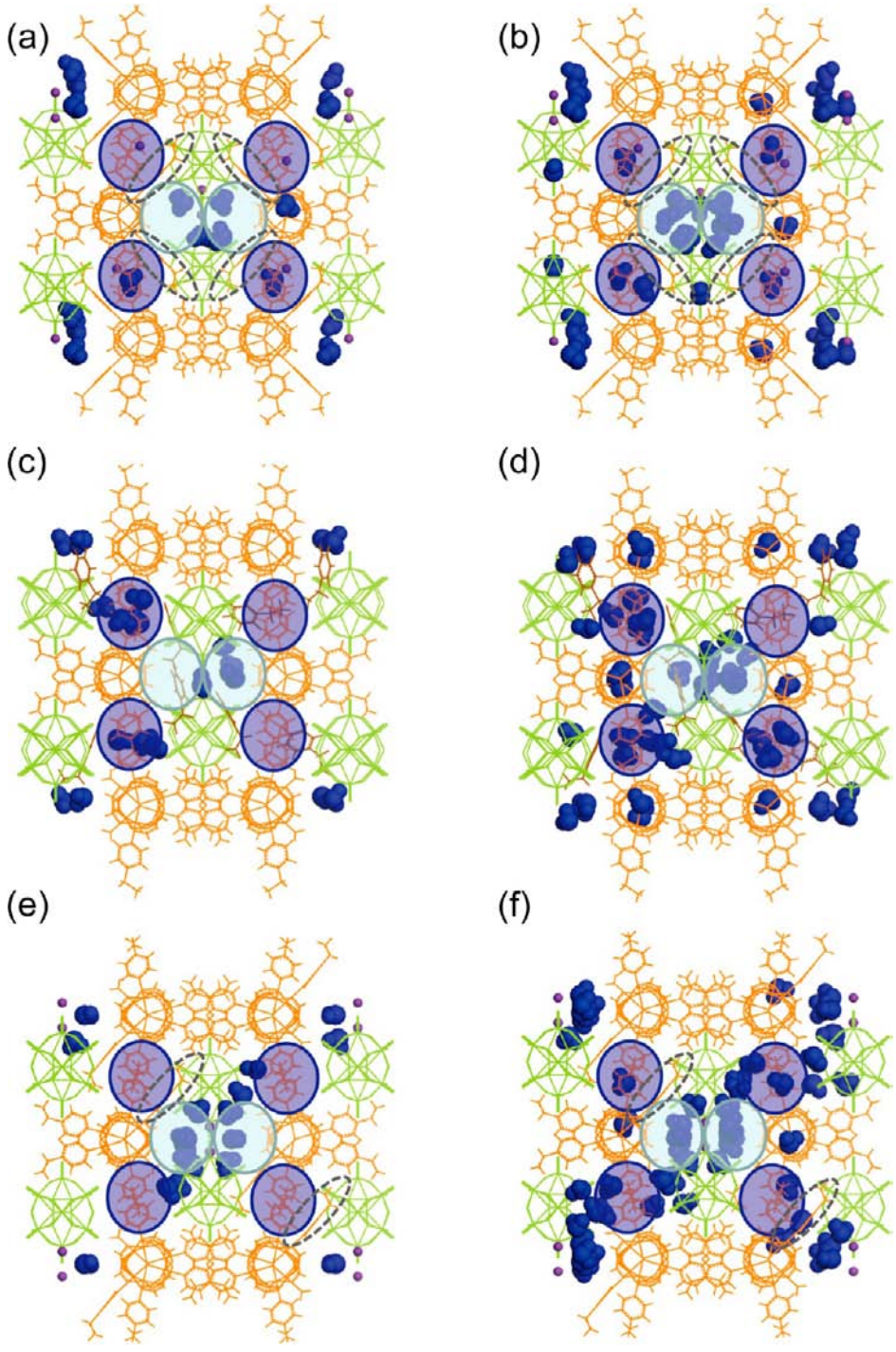

Figure 5. Typical optimized geometries of water molecules. (a) **1b** (2 mol mol^{-1}), (b) **1b** (6 mol mol^{-1}), (c) **2b** (2 mol mol^{-1}), (d) **2b** (8 mol mol^{-1}), (e) **3b** (2 mol mol^{-1}), and (f) **3b** (10 mol mol^{-1}). Light green and orange molecules show silicododecatungstates and macrocations, respectively. Purple spheres show K^+ ions. Brown molecules in (c) and (d) show etpyH$^+$ ions. Dark blue molecules show water. Transparent ovals show one-dimensional channels (light green, space I) and voids surrounded by etpy ligands (blue, space II). Gray broken ovals in (a), (b), (e), and (f) show the etpy ligands not involved in the $\pi-\pi$ interaction, which are removed and partially removed in **2b** and **3b**, respectively.

The K^+ ions in **1a** could be exchanged with Na^+ or Cs^+ ions without any structure changes by immersion of **1a** in an aqueous solution containing the corresponding nitrate salts, and $Na_2[Cr_3O(OOCH)_6(etpy)_3]_2[\alpha\text{-}SiW_{12}O_{40}]\cdot 8H_2O$ [**4a**] and $Cs_2[Cr_3O(OOCH)_6(etpy)_3]_2[\alpha\text{-}SiW_{12}O_{40}]\cdot 5H_2O$ [**5a**] were formed (see Supporting Information for details). Na^+ and Cs^+ ions were located in the one-dimensional channel of **4a** and **5a**, respectively, as in the case of **3a** (Figure S6 in the Supporting Information). Compounds **4a** and **5a** were treated in vacuo at 303 K, and their partially dehydrated compounds, $Na_2[Cr_3O(OOCH)_6(etpy)_3]_2[\alpha\text{-}SiW_{12}O_{40}]\cdot 2H_2O$ [**4b**] and $Cs_2[Cr_3O(OOCH)_6(etpy)_3]_2[\alpha\text{-}SiW_{12}O_{40}]\cdot H_2O$ [**5b**], respectively, were formed. Water sorption isotherms of **4b** and **5b** are shown in Figure 3b together with that of **1b**. The amounts of sorption for **4b** were largest in line with the largest ionic potential (z/r; z and r are the charge and radius of the ion,

dx.doi.org/10.1021/ic4008334 | Inorg. Chem. 2013, 52, 9320−9326

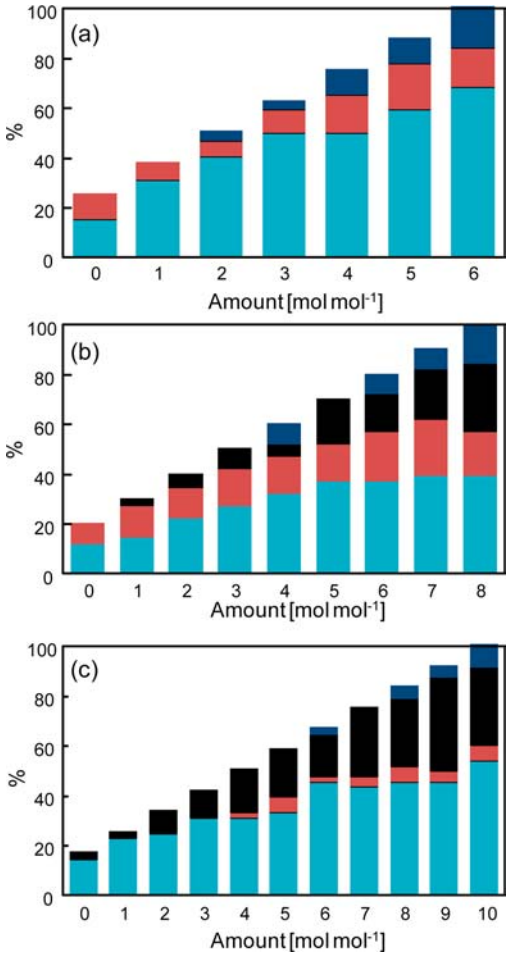

Figure 6. Amounts of water molecules in space I (light blue), space II (orange), space III (black), and other spaces (blue). The amounts are given in percentages based on the amounts of sorption at saturation as 100% for each compound. (a) **1b**, (b) **2b**, and (c) **3b**.

respectively) of Na^+.[16,17] Since polar water molecules generally interact with alkali metal ions via ion−dipole interaction,[18] these results suggest that alkali metal ions are water binding sites in the series of ionic crystals.

Alcohol and halocarbon sorption isotherms were also measured (Figure 4). The amounts of sorption for all compounds decreased in the order of methanol (cross-sectional area: 18 Å^2) > ethanol (23 Å^2) > dichloromethane (25 Å^2) > 1-propanol (27 Å^2) > 1,2-dichloropropane (32 Å^2), in line with increase in the guest molecule sizes (i.e., cross-sectional areas). Notably, while all compounds could sorb small amounts of 1-propanol (0.5−1.0 mol mol^{-1}), the amounts of 1,2-dichloropropane (<0.3 mol mol^{-1}) were comparable to that of surface adsorption, showing that 1,2-dichloropropane was excluded by all compounds. All these results suggest that the post-synthesis modification increases the pore volume and does not change the effective pore size.

MC simulations were carried out to investigate the water sorption sites. Typical water geometries sorbed in **1b** are shown in Figures 5a and 5b. Both at low amounts of sorption (Figure 5a) and at saturation (Figure 5b), water molecules were found mainly in the one-dimensional channels (space I) and resided in the vicinity of K^+ ions (K−O = 2.7−2.8 Å). Typical water geometries sorbed in **2b** are shown in Figures 5c and 5d. In contrast to **1b**, less than half of the water molecules were found in space I, and the rest were found in the voids surrounded by etpy ligands (space II) or the space created by the removal of etpy ligands (space III). The positions of water molecules in **2b** had no relevance to those of etpyH$^+$ ions. These results suggest that etpyH$^+$ ions do not work as water binding sites and probably hinder water sorption into space I. Typical water geometries sorbed in **3b** are shown in Figures 5e and 5f. At low amounts of sorption (Figure 5e), water molecules were found mainly in space I and resided in the vicinity of K^+ ions (K−O = 2.7−2.8 Å). At saturation (Figure 5f), water molecules were found in space III as well as space I. Figure 6 summarizes the amounts of water molecules in space I, space II, space III, and other spaces based on the amounts of water sorption at saturation as 100% for each compound. While the main location for water molecules is space I for all compounds, more than 30% of water molecules reside in space III of **3b** at saturation. The MC simulation results suggest that K^+ ions are strong water binding sites and removal of etpy ligands increases the water sorption capacity.

In order to confirm that K^+ ions are strong water binding sites, the amounts of K^+ ions in **3a** were controlled by the time of immersion of **2a** in the aqueous CH_3COOK solution, the resulting compounds were treated in vacuo at 303 K, and water sorption isotherms were measured (Figure S8 in the Supporting Information). The amounts of sorption at low vapor pressures increased with increase in amounts of K^+ ions, supporting that K^+ ions work as strong water binding sites.

■ CONCLUSION

Post-synthesis modification of a porous ionic crystal proceeded via two steps (acid treatment followed by ion-exchange) in an aqueous solution and a single-crystal-to-single-crystal manner. The porous ionic crystals of **1a** possessed one-dimensional channels, which can accommodate guests such as water, alcohols, and halocarbons. Crystals of **1a** were immersed in an aqueous HCl solution (acid treatment), the etpy ligand exposed to the one-dimensional channel was removed and exchanged with water, and **2a** was formed. Since K^+ ions, which are potential guest binding sites, were simultaneously removed by this treatment, reincorporation of K^+ ions was attempted by immersion of **2a** into an aqueous CH_3COOK solution (ion-exchange), and **3a** was formed. Increase in sorption capacity by the two-step post-synthesis modification was confirmed by sorption isotherms and Monte Carlo-based simulations using water as a probe molecule. The role of K^+ ions as water binding sites was confirmed by water sorption isotherms of alkali metal ion-exchanged compounds.

■ ASSOCIATED CONTENT

Ⓢ Supporting Information

Additional experimental methods and notes. IR spectra of **1a**, **2a**, and **3a** (Figure S1). Water sorption isotherms of **1b** and **1b′** (Figure S2). Photo images of the post-synthesis modification (Figure S3). Powder XRD patterns (experimental and calculated) of **2a**, **2b**, **3a**, and **3b** (Figure S4). Thermogravimetric analyses of **1b** and **3b** (Figure S5). Crystal structures of **4a** and **5a** (Figure S6). Amounts of water molecules in space I, space II, and other spaces of **4b** and **5b** (Figure S7). Water sorption isotherms at 298 K (the time of immersion of **2a** in the aqueous CH_3COOK solution was changed to control the amounts of K^+ ions) (Figure S8). This material is available free of charge via the Internet at http://pubs.acs.org.

dx.doi.org/10.1021/ic4008334 | Inorg. Chem. 2013, 52, 9320−9326

AUTHOR INFORMATION

Corresponding Author

*Tel: +81-3-5841-7272. Fax: +81-3-5841-7220 E-mail: tmizuno@mail.ecc.u-tokyo.ac.jp.

Present Address

†S.U.: Department of Basic Sciences, School of Arts and Sciences, The University of Tokyo, 3-8-1, Komaba, Meguro-ku, Tokyo 153-8902.

Notes

The authors declare no competing financial interest.

ACKNOWLEDGMENTS

This work was supported by the Japan Society for the Promotion of Science (JSPS) through its "Funding Program for World-Leading Innovative R&D on Science and Technology (FIRST Program), and Grants-in-Aid for Scientific Research from the Ministry of Education, Culture, Science, Sports, and Technology of Japan.

REFERENCES

(1) (a) Martínez, C.; Corma, A. *Coord. Chem. Rev.* **2011**, *255*, 1558. (b) Horike, S.; Shimomura, S.; Kitagawa, S. *Nat. Chem.* **2009**, *1*, 695. (c) Tranchemontagne, D. J.; Ni, Z.; O'Keeffe, M.; Yaghi, O. M. *Angew. Chem., Int. Ed.* **2008**, *47*, 5136.

(2) (a) Velu, S.; Ma, X.; Song, C. *Ind. Eng. Chem. Res.* **2003**, *42*, 5293. (b) Chen, H. Y.; Sun, Q.; Wen, B.; Yeom, Y. H.; Weitz, E.; Sachtler, W. M. H. *Catal. Today* **2004**, *96*, 1.

(3) (a) Kim, M.; Cahill, J. F.; Fei, H.; Prather, K. A.; Cohen, S. M. *J. Am. Chem. Soc.* **2012**, *134*, 18082. (b) Yamada, T.; Kitagawa, H. *J. Am. Chem. Soc.* **2009**, *131*, 6312. (c) Wang, Z.; Cohen, S. M. *J. Am. Chem. Soc.* **2007**, *129*, 12368. (d) Zhu, W.; He, C.; Wu, P.; Wu, X.; Duan, C. *Dalton Trans.* **2012**, *41*, 3072.

(4) (a) Beauvais, L. G.; Shores, M. P.; Long, J. R. *Chem. Mater.* **1998**, *10*, 3783. (b) Takamizawa, S.; Akatsuka, T.; Ueda, T. *Angew. Chem., Int. Ed.* **2008**, *47*, 1689.

(5) Reviews on POMs. (a) Pope, M. T.; Müller, A. *Angew. Chem., Int. Ed. Engl.* **1991**, *30*, 34. (b) Okuhara, T.; Mizuno, N.; Misono, M. *Adv. Catal.* **1996**, *41*, 113. (c) Hill, C. L. *Chem. Rev.* **1998**, *98*, 1. (d) Neumann, R.; Khenkin, A. M. *Chem. Commun.* **2006**, *24*, 2529. (e) Long, D. L.; Burkholder, E.; Cronin, L. *Chem. Soc. Rev.* **2007**, *36*, 105.

(6) (a) Uchida, S.; Mizuno, N. *J. Am. Chem. Soc.* **2004**, *126*, 1602. (b) Uchida, S.; Kawamoto, R.; Tagami, H.; Nakagawa, Y.; Mizuno, N. *J. Am. Chem. Soc.* **2008**, *130*, 12370. (c) Eguchi, R.; Uchida, S.; Mizuno, N. *J. Phys. Chem. C* **2012**, *116*, 16105. (d) Uchida, S.; Lesbani, A.; Ogasawara, Y.; Mizuno, N. *Inorg. Chem.* **2012**, *51*, 775. (e) Mizuno, N.; Uchida, S.; Kamata, K.; Ishimoto, R.; Nojima, S.; Yonehara, K.; Sumida, Y. *Angew. Chem., Int. Ed.* **2010**, *49*, 9972.

(7) Eguchi, R.; Uchida, S.; Mizuno, N. *Angew. Chem., Int. Ed.* **2012**, *51*, 1635.

(8) McClellan, A. L.; Harnsberger, H. F. *J. Colloid Interface Sci.* **1967**, *23*, 577.

(9) Metropolis, N.; Rosenbluth, A. W.; Rosenbluth, M. N.; Teller, A. H.; Teller, E. *J. Chem. Phys.* **1953**, *21*, 1087.

(10) Rappé, A. K.; Casewit, C. J.; Colwell, K. S.; Goddard, W. A., III; Skiff, W. M. *J. Am. Chem. Soc.* **1992**, *114*, 10024.

(11) Mulliken, R. S. *J. Chem. Phys.* **1955**, *23*, 1833.

(12) Delley, B. *J. Chem. Phys.* **2000**, *113*, 7756.

(13) Perdew, J. P.; Burke, K.; Ernzerhof, M. *Phys. Rev. Lett.* **1996**, *77*, 3865.

(14) Li, J. R.; Kuppler, R. J.; Zhou, H. C. *Chem. Soc. Rev.* **2009**, *38*, 1477.

(15) Gregg, S. J.; Sing, K. S. W. *Adsorption, Surface Area, and Porosity*; Academic Press: London, 1967.

(16) Ionic radii of Na^+, K^+, and Cs^+ ions are 1.18, 1.51, and 1.81 Å, respectively,[17] and Na^+ shows the largest ionic potential.

(17) Shannon, R. D. *Acta Crystallogr., Sect. A* **1976**, *32*, 751.

(18) Dzhigit, O. M.; Kiselev, A. V.; Mikos, K. N.; Muttik, G. G.; Rahmanova, T. A. *Trans. Faraday Soc.* **1971**, *67*, 458.